OPEN ACCESS

Study the effect of perforation type for plate with central crack on the stress intensity factor using the XFEM

Ahmed Obaid Mashjel [1,*], Rafil Mahmood Laftah [2], Hassanein Ibraheem Khalaf [3]

[1,2,3]*Department of Mechanical Engineering, College of Engineering, University of Basrah, Basrah, Iraq*
E-mail addresses: ahmedobaid86@gmail.com , rafil.laftah@uobasrah.edu.iq , hassanein.khalaf@uobasrah.edu.iq

Abstract

In this study, loading was carried out for several types of perforated plates, such as circular, rhombic and rectangular holes, where the holes were arranged in two types, namely straight arrangement and alternating arrangement. The stress intensity factor and shape factor were calculated for each case, taking into account the diameter of the holes. So, it is found the SIF increases significantly when the plate is perforated, and the same applies to the shape factor, also increases. In the case of circular holes, the increases in the average value of (SIF) reached to (80.88 %) when the plate was perforated with alternated arranged of circular holes, while the straight arrangement of circular holes the increases of average values of SIF reach to (67.55 %). Either in the case of rhombus holes: the SIF values are increases to (51.07 %) when the plate was perforated with the alternated arrangement, while in the straight arrangement of holes the (SIF) increase to (35.43 %). It was observed through this study, the increases of stress intensity factor and the shape factor with different crack lengths were more stable in the plate that perforated with an alternated arrangement of holes than the straight arrangement. The higher values of stress intensity factor obtained when the plates were perforated with circular holes, due to the circular shape has more stiffness, so the Absorption of force will be small Compared with the rhombus and rectangular shape that will be less stiffness which the absorption of strength is greater.

Keywords: crack, perforated plate, stress intensity factor, shape factor, ABAQUS.

Nomenclature	
a	Half crack length (mm)
E	Young's modulus (Pa)
G	Energy release rate
KI	Stress intensity factor (MPa)
w	Width of plate (mm)
XFEM	Extended finite element method
Y	Shape factor
Greek symbols	
σ	Normal stress (pa)
υ	Poisson's ratio

1. Introduction

Over the earlier decenniums the perforated plate has found growing application in modern pressure vessels and heat exchangers in addition to the nuclear reactors, as these plates compose an essential part in the power plant process and chemical processing refineries. The process of perforation of metal plates is presented in the industry for more than a hundred and fifty years. In the beginning, the process was conducted manually using simple tools like hammer and cutting tools to remove parts of metallic plates. Recently the process of perforation of plates becomes much more accurate and efficient with the use of CNC and laser technology [1, 2]

Recently perforated plates have many uses in industrial and architectural applications. This encourages the manufactures to produce this type of plates with low cost and high mechanical properties and weight factors.

In architectural applications, the perforated plates are commonly used as a sunshade, cladding panel, safety barrier, and walls covering. In applications like energy and chemical process perforated plates plays an important role in the construction of heat exchangers [3], gas detergent and, the basin of washing machine as well as colanders and steam generators. In automotive applications, perforated plates are being used as air and gas candidates. In construction applications perforated plated are found in noise insulators, stairs barriers and sun umbrellas [2, 4].

R. Bailey [5], introduced a theoretical method to investigate the elastic behavior of the plate that loaded at the ends. Closely spaced circular holes are cut in the plates forming a square as well as a diagonal pattern.

The general technique of solution was established experimentally for different loading conditions. Absolute solutions have been reached for the distribution of stress in plates that contain holes. These results have been used to find design curves for Young's modulus, shear modulus, Poisson's ratio, and stress concentration factors for plates with square or circular holes. R. Bailey and R. Hicks, (1960) [6] were presented a new technique to define the elastic conductance for the perforated plate with circular holes that arranged alternately or straight patterns. This technique of solution has been confirmed by experimental work for various types of loading. Integral solutions have been achieved for the

distribution of stress in plates that perforated with circular holes with various ratios of (pitch to diameter) by using a digital computer, the solutions that obtained used to find the design curve of effective share and young modulus, Poisson's ratio and stress concentration factors. It is suggested to find a convergent solution by using a limited number of factors such as stress and displacement elements and verify the boundary conditions around the edges of plate. S. MALL and J. C. NEWMAN,

JR (1986) [7], presented solutions to the SIF of the crack that produced from a hole having a circular shape that undergo various conditions of the loading, by using a boundary-collocations analysis to find the stress intensity factor of two cracks that produced from circular holes, and finding the equations of displacement of the crack's surfaces. This is very important to improve the analysis of fracture analysis under monotonic load based on the tip of opening crack displacement (CTOD), and improve the (crack-closure) models to find the crack growth that is produced from a hole under cyclic of Load. Mihir M Chauhan et al. (2015) [8] exhibited a new approach to determine the stress intensity factor for a circular hole in plate undergo loading plan. The approach based on the derivation of a series form of the of complex stress function via the complex variables approach is integrated with the boundary collocation method. They showed how the value of SIF is affected by variation of factors like plate dimensions, properties of materials, holes geometry and type of loading.

The (ABAQUS) software uses the principles of the Extended Finite Element Method (XFEM) to calculate the values of the SIF. XFEM is used to find SIF in perforated plates with different shapes and sizes of holes and arrangement of these holes and then to calculate the fracture toughness. This requires finding SIF in the crack tip. By XFEM, functions of discontinuous enrichment were added to the finite element approximation to account for the presence of the crack. The discontinuity is independent of the mesh, and at the variance of FEM, there is no need to re-meshing the crack domain [9].

Studying the effects of length of the crack as well as the size and shapes of the perforation on the SIF and geometry factor Y, was the main objective of this study
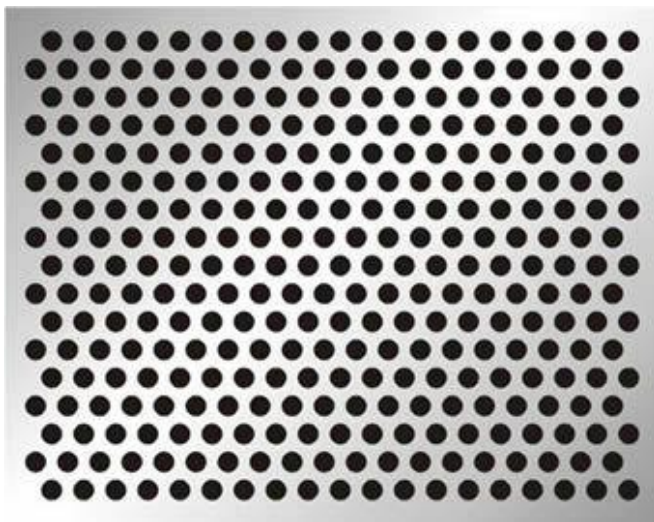

Fig. 1 Perforated metal plate.

2. Extended Finite Element Method (XFEM)

The XFEM is a numerical technique which depends on method of approximation which called (enrichment), which

comes in the prior knowledge of the solution. This means these discontinuities; high gradients and singularities can be approximated directly through the technique of the enrichment autonomously of generation mesh. The enrichment is defined in a local area through the introduction of enrichment functions and corresponding additional degrees of freedom, so these degrees of freedom were ordinarily realized in the respective nodes i.e. enrichment can be realized on the basis of node. The approximation of the XFEM is obvious concept and simple to formulate. Moreover, XFEM can be easily executed through simple modification of the standard codes of the FEM with the similar framework [10].
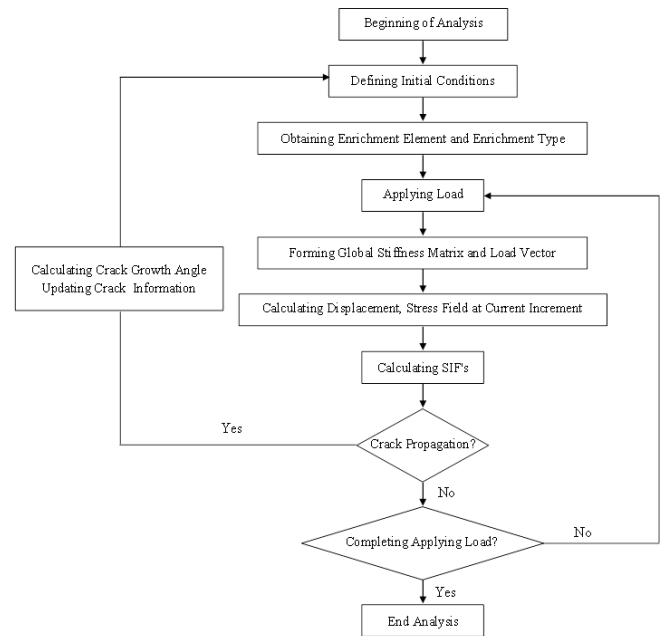

Fig. 2 the XFEM Flow diagram [13].

3. Extended Finite Element Formulation

The XFEM has an essential concept that is to enriching of the approximation domain, therefore it is capable of propagating some features of the issue of interest, in certain discontinuities like the cracks and interfaces region. In spite of the fact that it is a local version of the PUFEM enrichment utilized exclusively in a clear local domain, it has been highly reckon on the evolution of external enrichments for crack modelling by several of Meshless like (EFG) and (Hp-clouds). The main approximations of the XFEM have been developed for modelling the robust discontinuities in fracture mechanics problems. This has been later extended to comprise the weak discontinuity and interface issues [11].

The function of enrichment approximation u(x) is presented in Eq. (1).

$$u^h(x) = u^{FE} + u^{enr} = \sum_{j=1}^{n} N_j(x)u_j + \sum_{k=1}^{m} N_k(x)\psi(x)a_K$$

(1)

The $N_i(x)$ refer to the usual nodal shape functions, u_j is the vector of uniform degrees of nodal freedom in the FEM, a_K is the additional set of degrees of freedom to the classical FE model and $\Psi(x)$ is the function of discontinuous enrichment [12].

4. The Stress Intensity Factor

In fracture mechanics the (SIF) have been used to predict the intensity of the stress or stress concentration at the crack tip and notch due to a remote loading of residual stresses. The (SIF) is a theoretical value commonly applied to a homogeneous and linear elastic fracture mechanics (LEFM) material and is advantageous for providing criteria of the failure for fragile materials. The determination of the (SIF) may also potential through its definition that relates it to field of the stress, and stress components must calculate carefully upon which (KI) results from extrapolation to the tip of a crack. Due to the stresses that are studied in integration points and the tip of the crack is located in an element node, this calculation is not exactly according to the definition of stress intensity factor (KI). It always remains to be investigated how the interpolation has to be done to get the best results [13].

Stress field and displacement which close to the tip of the crack have been considered as of important parameters to investigate the (SIF) values in linear elastic fracture mechanics via FE analysis, by using these parameters to predict the propagations of the crack and the failures under specific load conditions. A number of methods have been used to calculate the values of the (KI), such as the virtual crack extension method, J- integral and displacement correlation methods. The computational evaluation of the (SIF) may be categorized as direct approach and energy approach. The direct approach relates the (SIF) with the results of FE technique, while the second approach depends on the calculation value of the (G) [14].

The function of the stress distribution near the tip of the crack [15] is given by:

$$\sigma_{yy} = \frac{K_I}{\sqrt{2\pi a}} + \cos\frac{\theta}{2}\ (1 + \sin\frac{\theta}{2}\sin\frac{3\theta}{2}) \tag{2}$$

$$\sigma_{xx} = \frac{K_I}{\sqrt{2\pi a}} + \cos\frac{\theta}{2}\ (1 - \sin\frac{\theta}{2}\sin\frac{3\theta}{2}) \tag{3}$$
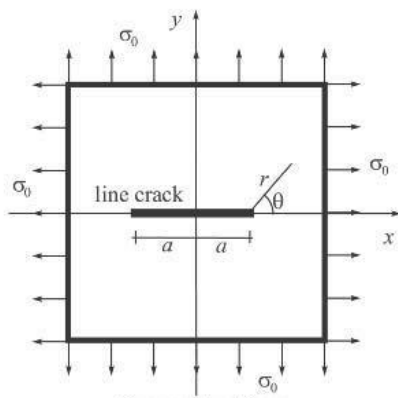

Fig. 3 Flat plate with central crack.

Where, (r) is refers to the range from the crack tip, and θ is refers to the orientation. When the stress distribution in crack plane, the orientation parameter (θ) becomes zero and Eq. (2) and (3) will be reduced to Eq. (4) and (5):

$$\sigma_{yy} = \frac{K_I}{\sqrt{2\pi a}} \tag{4}$$

$$\sigma_{xx} = \frac{K_I}{\sqrt{2\pi a}} \tag{5}$$

5. Properties and Dimensions of the Plate

The plates used in the study are made from carbon steel with Young's modulus is 210 GPa and Poisson's ratio (0.3 - 0.33). It contains circular holes with different sizes distributed by alternated and straight arrangement as shown in Figures 4 and 5. Table 1 refers to the dimensions of the perforated plate used in this study.
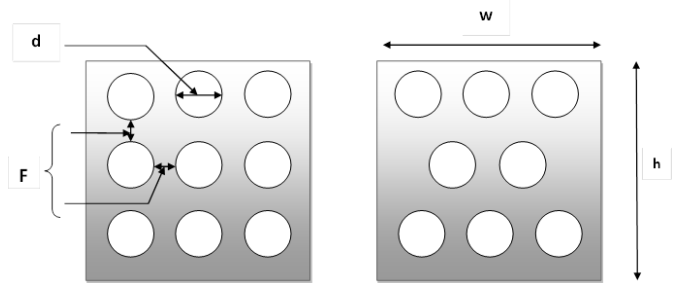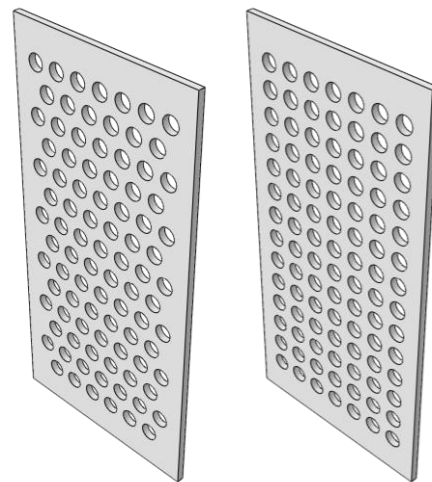

Fig. 4 Perforated plate dimensions.

Fig. 5 the geometry of perforated plates.

Table 1 Dimensions of perforated plate with circular holes.

Symbol	h	w	t	d
Dimension	240 mm	120 mm	4 mm	5, 10, 15 mm

A theoretical solution of the (SIF) in flat plate containing a central crack maybe calculated via Eq. (6) and (7) [16].

$$K_I = Y\sigma\sqrt{\pi a} \tag{6}$$

$$Y = 1 + 0.256(a/w) - 1.152(a/w)^2 + 12.2(a/w)^3 \tag{7}$$

$$K_n = \sigma\sqrt{\pi a} \tag{8}$$

Where, (Y) is the shape factor.

The analytical and numerical values of SIF of the central cracked plate under uniform pressure (1 MPa) are plotted against (a/w) for twelve crack length (10 to 120 mm) with step 10 mm as shown in Fig. 7. The results show good agreement between the analytical and numerical solution. It also could be noted from this figure that the value of Von Mises stress decrease when moving from the crack tip because the stress is concentrated at the tip of crack and less when moving from the tip of crack to the plate's boundaries. Fig. 6 represents the stress around the crack tip for flat plate.

Additionally, the holes will alter the stress distribution in the plate, so the stress concentration may increase in certain areas and decrease in others. Therefore, the SIF will be different with the changing of crack length. So, at the areas with less stress concentration, the SIF will decrease and vice versa. This figure also shows that the diameters of the holes (10 and 15 mm) make the increasing and decreasing of the values of the SIF more stable than the 5 mm diameter. Figure 8 represent the stress distribution around the crack tip in the perforated plates with the alternated arrangement of holes.
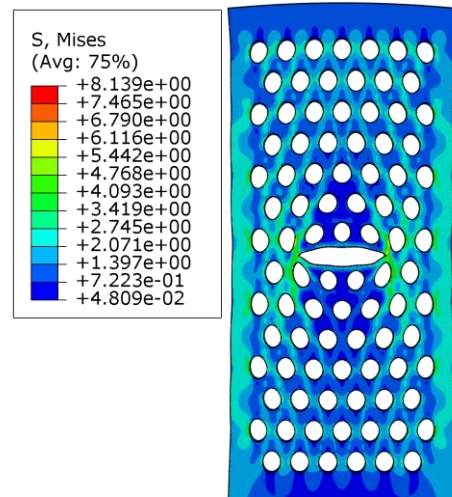

Fig. 6 Stress distribution fringes.

Fig. 8 Stress distribution fringes in perforated plate with alternated arrangement of holes.

Fig. 7 theoretical and XFEM of stress intensity factor that effected by different length of the crack.

Fig. 9 Effect of crack length on the SIF in perforated plates with alternated arrangement of holes.

6. Effect of the Shape and Size of Perforations on the (SIF) KI

6.1. Perforated Plate with Central Crack

Case 1: Plate Containing a Circular Perforation.

Figure 9 shows the values of the SIF against the ratio of (a/w) for the perforated plates with alternated arrangement of holes (5, 10 and 15 mm diameter) With five various lengths of the crack (10 to 50 mm) by 10 mm step. It is noted from this figure that the value of stress intensity factor increase and decrease significantly when the plates have a perforations, but it remains stable with gradual rising in the non-perforated plates, due to material stiffness and plate geometry, while the cutting holes lead to a decrease in the weight of the plate and this will cause a reduction of the mass moment of inertia value, which in turn leads to a reduction in the stiffness of the plate,

In the case of the straight arrangement of the perforations as shown in Fig. 11, it is noted that the stability in the increasing value of the stress intensity factor may be obtained in the plate with small diameter of perforations (5 mm) while the plate with holes of (10 mm) comes after, in the stability of the SIF values. Also, it is noted that the values of the SIF increase significantly in the plates which have perforated with (15 mm) holes diameter. Figure 10 represent the stress distribution around the crack tip in the perforated plates with the straight arrangement of holes.

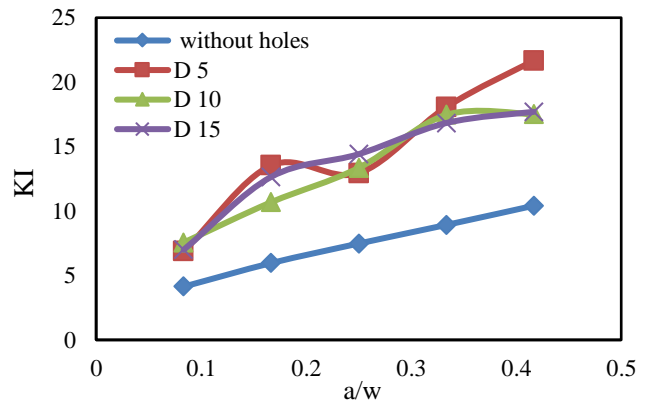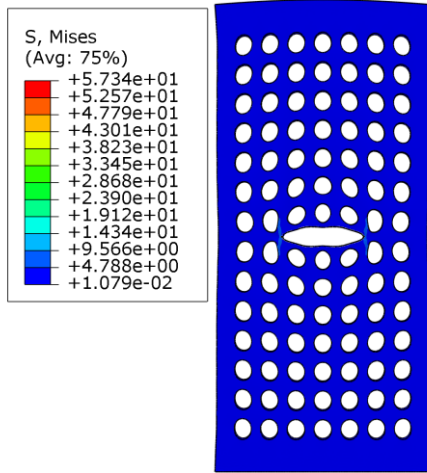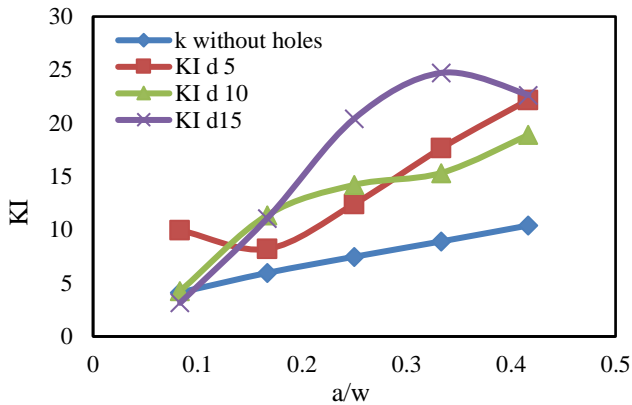**Fig. 10** Stress distribution fringes in perforated plate with straight arrangement of holes.

Fig. 11 Influence of crack length on the SIF in perforated plate with straight arrangement of holes.
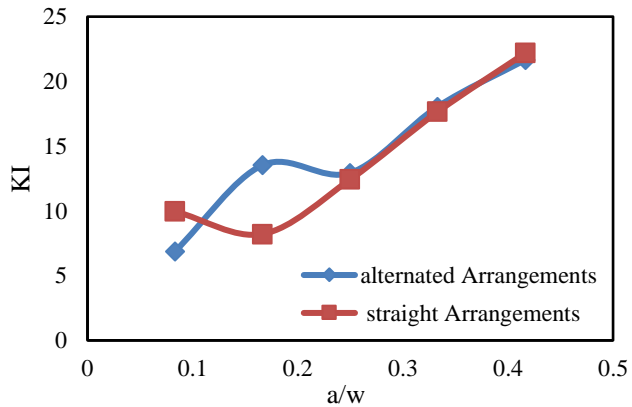

Fig. 12 Effect of crack length on the SIF in perforated plate with alternated and straight arrangement of 5 mm hole diameters.
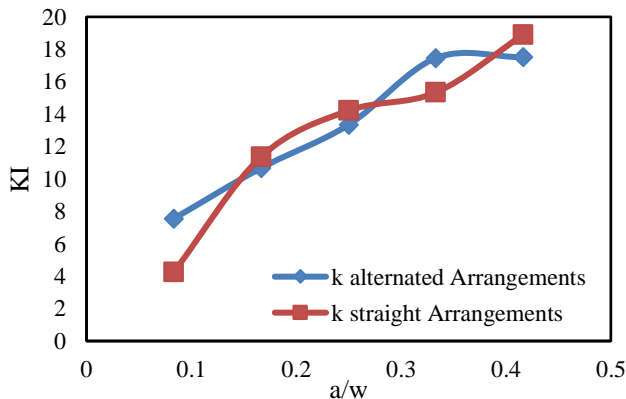

Fig. 13 Effect of crack length on the SIF in perforated plate with alternated and straight arrangement of 10 mm hole diameters.
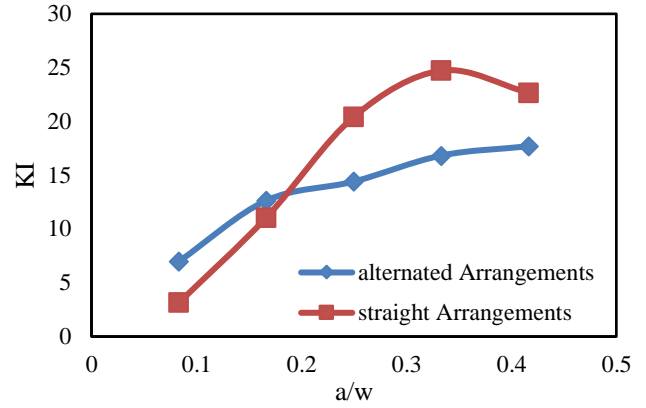

Fig. 14 Effect of crack length on the SIF in perforated plate with alternated and straight arrangement of 15 mm hole diameters.

Figures 12, 13 and 14 present the values of SIF which are obtained numerically depending on the XFEM concepts by using program software ABAQUS, plotting of SIF values against to the ratio of crack length to width of plate (a/w) for the two types of the arrangement which are dependent used in this study (alternated and straight arrangement). It is noted that from these figures that the SIF values in the plate with the straight arrangement of perforation are increased significantly and higher than of its value in the other arrangement which is alternated, the higher value of the stress intensity factor may be obtained in the plate with 15 mm diameter of the perforation with the straight arrangement.

The effect of shape factor for different diameter of holes is shown in Fig. 15 and presented in Eq. (9) obtained from curve expert program with correlation factor (r^2 = 91.13 %). It is noted that from figures that the SIF and shape factor more stable when diameter of holes 10 mm.
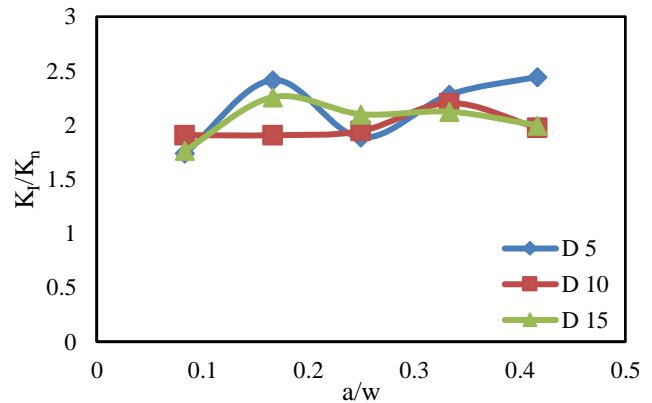
Where, $Y = K_I / K_n$

Fig. 15 Effect of crack length on shape factor Y for the alternated arrangement of circular hoes of perforated plate.

$$Y((a/w), D) = -29299.316 + 8.385\,(a/w) - 29.228\,(a/w)^2 + 45.783\,(a/w)^3 + 10743.596\,(D) - 1172.032\,(D)^2 + 39.067\,(D)^3 + 0.0246\,(a/w)(D) - 0.987\,(a/w)^2(D) + 0.0177\,(a/w)(D)^2 \qquad (9)$$

In the case of straight arrangement holes, the effect of different diameter of holes on the shape factor is clear as shown in Fig. 16 with equation (10) that obtained from curve expert program.
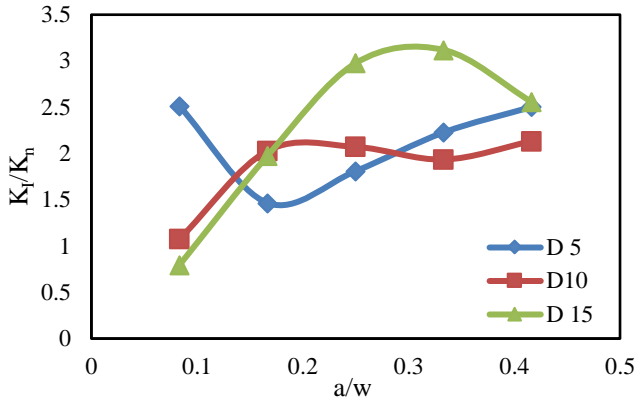
Fig. 16 Effect of crack length on shape factor Y for the straight arrangement of circular hoes of the perforated plate.

$$Y((a/w), D) = 35987.56 - 35.98\,(a/w) + 90.3\,(a/w)^2$$
$$- 38.685\,(a/w)^3 - 13193.749\,(D) + 1439.26\,(D)^2$$
$$- 47.975214\,(D)^3 + 3.448\,(a/w)(D) - 7.267\,(a/w)^2(D)$$
$$+ 0.0327\,(a/w)(D)^2 \qquad\qquad (10)$$

The equations (9) and (10) are available when ($F = d/2$)

Case 2: Plate with Rhombus Holes:

In this case, the plates have been perforated with rhombus holes with three different side size includes (3.13 mm, 6.65 mm, and 9.38 mm) which also arranged by straight and alternated arrangement as Fig. 17, where Fig. 17(a) represent the straight arrangement while Fig. 17(b) represent the alternated arrangement, Table 2 represents the dimensions of perforated plate with rhombus holes. Fig. 25 represent the geometry and dimensions of the rhombus hole.

Figure 19 is presents a schematic diagram of the SIF against the ratio of (a/w) for the perforated plates with alternated arrangement of rhombus holes (3.13, 6.65 and 9.38 mm side size with five various lengths of the crack (10 to 50 mm) taking into consideration with 10 mm step for each increase of the length of cracks, it is observed that from this figure that the values of the SIF are increased significantly when the rhombus perforations are made in the plate, but it remains stable with gradual rising in the non-perforated plates that due to material stiffness and plate geometry as mentioned before in the case of circular holes. Also, it is noted that from this figure that the smaller the size of the holes, the higher the values of the SIF. It can clearly observe that the highest SIF values in plates with side size of rhombus holes (3.13 mm), while the others size (6.65 and 9.38 mm) it comes after. Figure 18 represents the stress distribution fringes around the crack tips.

Table 2 Dimensions of perforated plate with rhombus holes.

Symbol	h	w	t	L
Dimension	240 mm	120 mm	4 mm	(3.13, 6.65, 9.38) mm

The angles between the sides of rhombus hole ($\alpha = 73.74°$), ($\beta = 106.26°$)
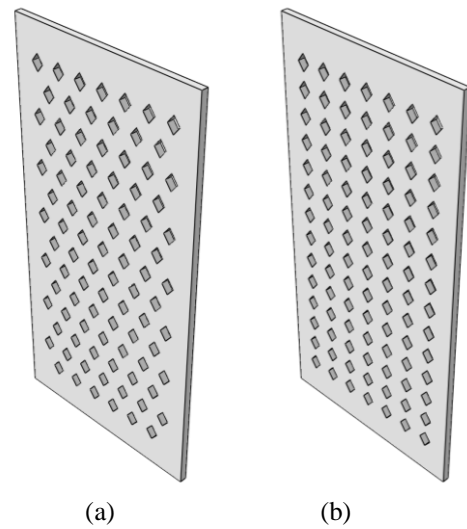

(a)   (b)

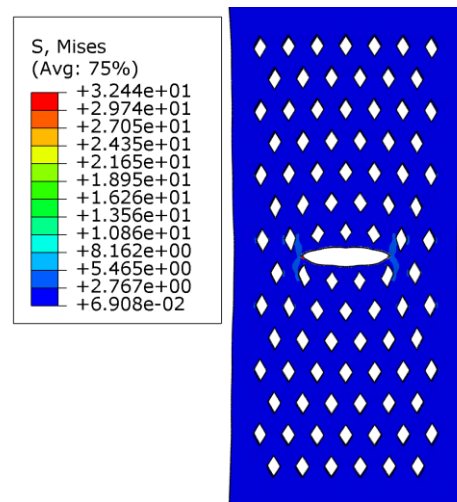**Fig. 17** the geometry of perforated plates with rhombus perforations.

Fig. 18 Stress distribution fringes in perforated plate with alternated arrangement of rhombus holes.
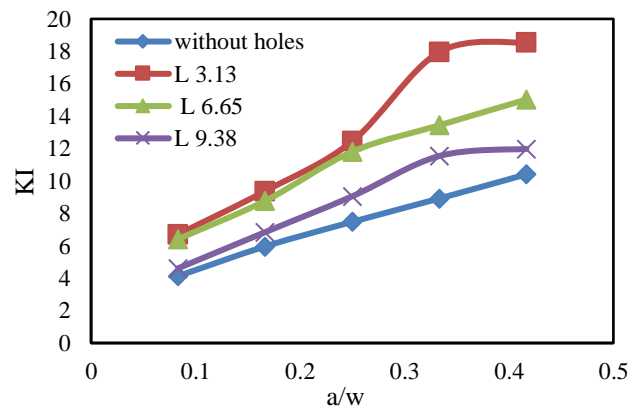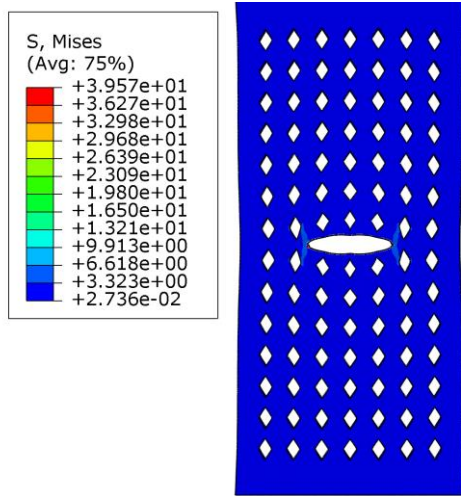

Fig. 19 Effect of crack length on the SIF in perforated plates with alternated arrangement of rhombus holes.

In the straight arrangement case of the rhombus perforations as shown in Fig. 21 it is noted that the stability in the increasing value of the stress intensity factor may be obtained in the perforated plates with rhombus side size (6.65 and 9.38 mm) while the plate which has the rhombus perforation (3.13 mm) increased significantly in the values of the stress intensity factor and reach to the maximum values at crack length (50 mm). In general, this type of arrangement of

perforations leads to lead to a higher increasing of the stress intensity factor values that were drawn against to the ratio of the crack length to specimen width (a/w) compared with the alternating arrangement which is more stable. The stress distribution (fringes) of the crack tip for the perforated pales with alternated arrangement of hoes is represented in Fig. 20. Figures 22, 23 and 24 represent the curves of the stress intensity factor against the ratio (a/w) for the straight and alternated arrangement respectively.

Fig. 20 Stress distribution fringes in perforated plate with straight arrangement of rhombus holes.
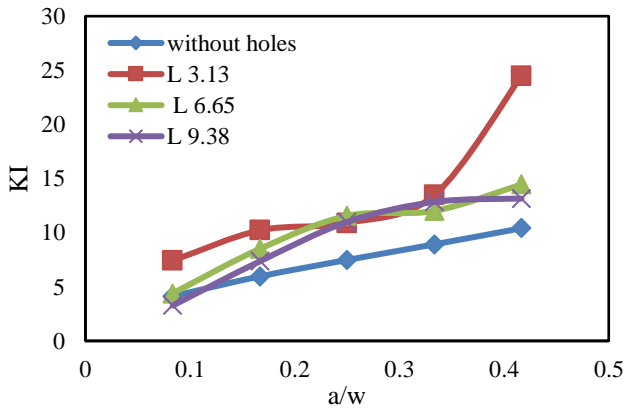

Fig. 21 Effect of crack length on the SIF in perforated plates with straight arrangement of rhombus holes.
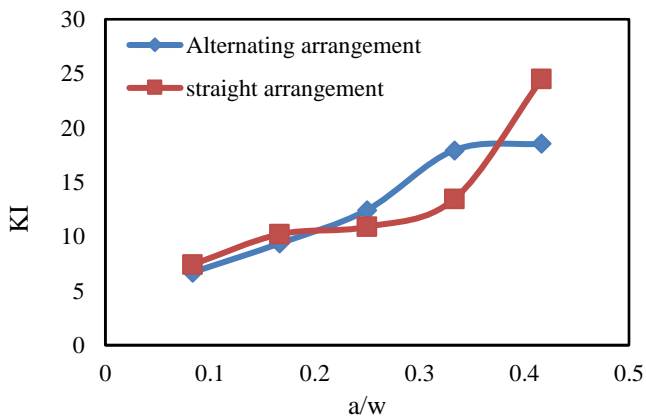

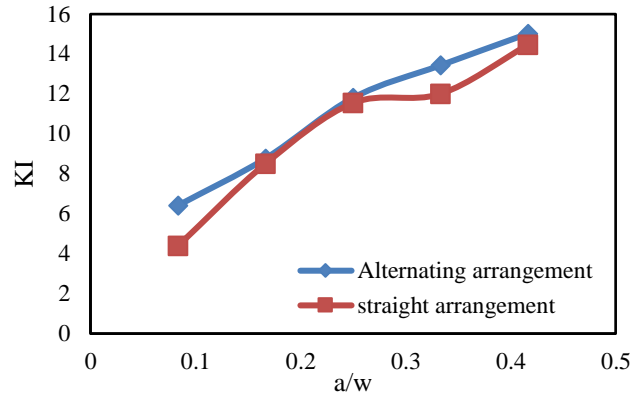**Fig. 22** Effect of arrangements of (L = 3.13 mm) on the SIF K_I

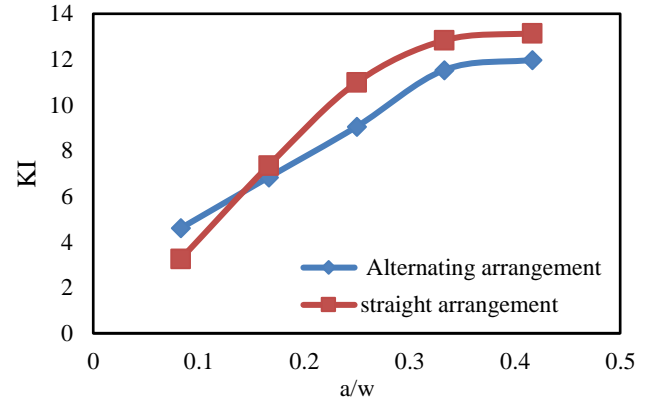**Fig. 23** Effect of arrangements of (L = 6.65 mm) on the SIF K_I

Fig. 24 Effect of arrangements of (L = 9.38 mm) on the SIF K_I

The effect of shape factor for different Length of sides (L) of the rhombus holes is shown in Fig. 26 and presented in Eq. (11) that obtained from the curve expert program with correlation factor. It is noted that from figures that the SIF and shape factor more stable when side length (L) of rhombus holes increase.
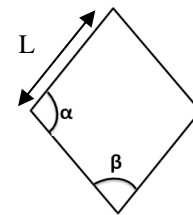

Fig. 25 Dimensions of rhombus hole.

$$Y((a/w), L) = 40654.299 - 8.334\,(a/w) + 43.873\,(a/w)^2 - 60.097\,(a/w)^3 - 23434.863\,(L) + 3989.407\,(L)^2 - 208.216\,(L)^3 \qquad (11)$$

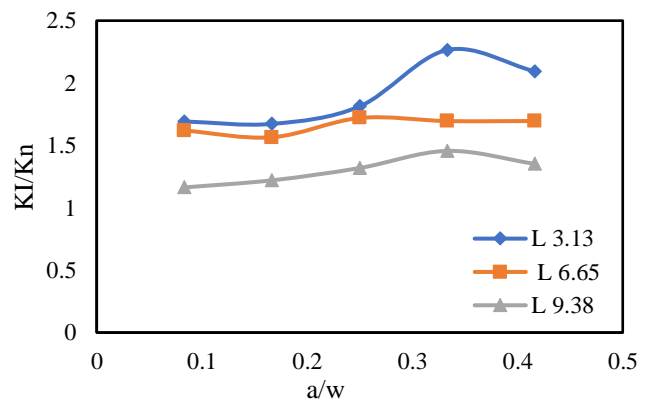This equation is available for ($\alpha = 73.74°$), ($\beta = 106.26°$)

Fig. 26 Effect of crack length in plate with alternated arrangement of rhombus holes of the perforated plate on shape factor Y.

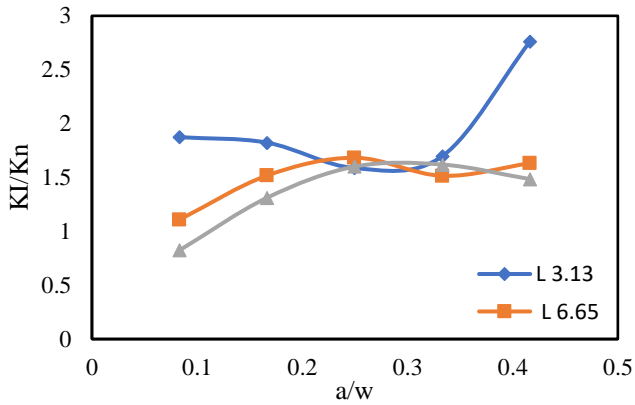Figure 27 show the effect of straight arrangement holes on the shape factor (Y) that can be found from the Eq. (12).

Fig. 27 Effect of crack length in plate with straight arrangement of rhombus holes of the perforated plate on shape factor Y.

$$Y((a/w), L) = 10236.61 - 4.642\,(a/w) - 17.023\,(a/w)^2$$
$$+ 82.191\,(a/w)^3 - 5899.8\,(L) + 1004.28\,(L)^2$$
$$- 52.415\,(L)^3 + 2.515\,(a/w)(L) - 6.9\,(a/w)^2(L) +$$
$$0.0746(a/w)(L)^2 \qquad (12)$$

6.2. Plate with Rectangular Holes

Figure 31 is representing the plotting curve of the SIF against the ratio of (a/w) for the perforated plates with alternated arrangement of rectangular holes with five various lengths of the crack (10 to 50 mm) by 10 mm steps of increase. It is noted that from this figure that the value of stress intensity factor are decreases when making a rectangular perforation in the plates except the size of (S = 5 mm) it makes the values of the SIF increase significantly. But it remains stable with gradual rising in the non-perforated plates due to material stiffness and plates geometry as mentioned before in the case of circular holes.

It also clearly showed by this figure the significant dissimilar in the rising and the lowering the values of the SIF. Fig. 28 refers to the geometry of the perforated plate with rectangular holes. Fig. 30 represent the stress distribution around the crack tip in the perforated plates with the alternated arrangement of holes.
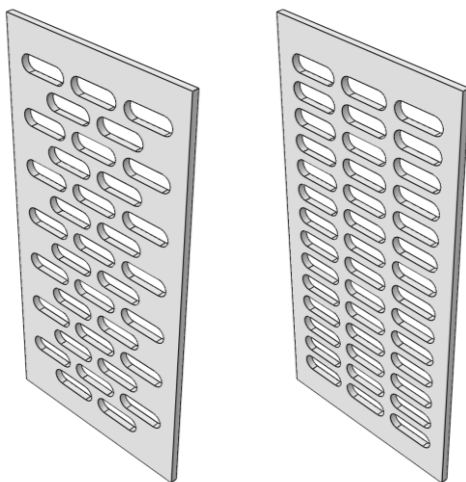

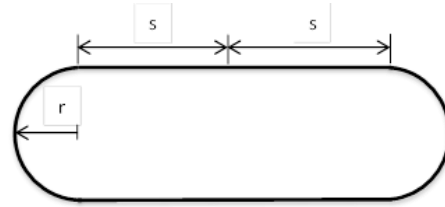**Fig. 28** the geometry of perforated plates with rectangular perforations.

Fig. 29 Dimensions of rhombus hole.

Table 3 dimensions of perforated plate with rectangular holes.

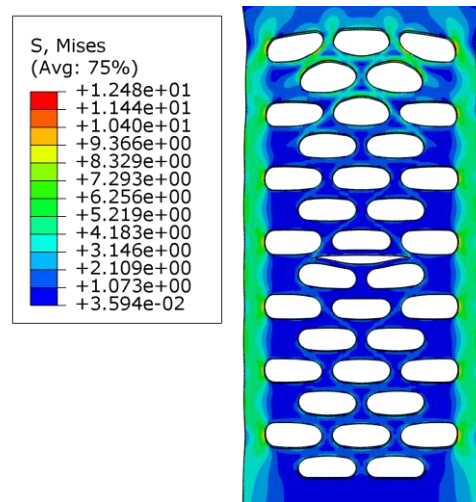| Symbol	h	w	t	r
Dimension	240 mm	120 mm	4 mm	(2.5, 5, 7.5) mm

The values of (S = 2r).

Fig. 30 Stress distribution fringes in perforated plates with alternated arrangement of rectangular perforations.
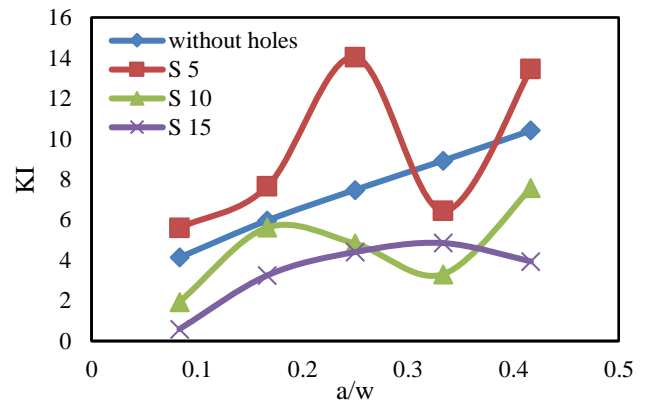

Fig. 31 Influence of crack length on the SIF in perforated plates with alternated arrangement of rectangular perforations.

For the case of the straight arrangement of the perforations as shown in Fig. 33. It was observed that the stress intensity factor values in the perforated plate with holes size (S = 5 and S = 15) start at less than their value in the non-perforated plate, and then begin to rise to reach their highest value at the middle of the crack length but its start decreasing until it reaches its lowest value at the longer crack length, while the plate which has been perforated with holes size (S = 10) make the values of the stress intensity factor increase gradually. Fig. 32 represent the stress distribution around the crack tip in the perforated plates with the straight arrangement of holes.

Figures 34, 35 and 36 represent the curves of the stress intensity factor against the ratio (a/w) for the straight and alternated arrangement respectively.
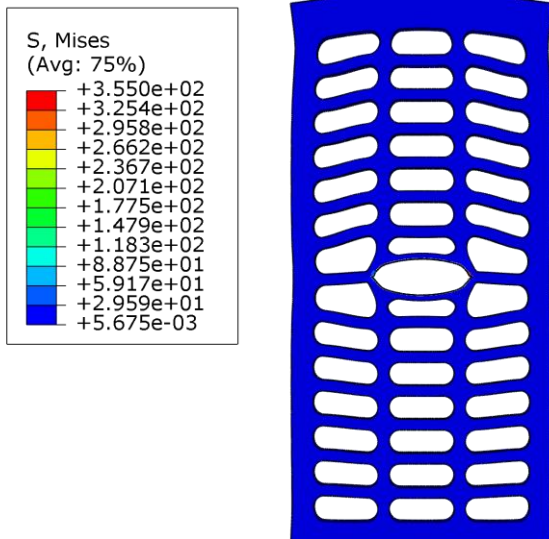

Fig. 32 Stress distribution fringes in perforated plates with straight arrangement of rectangular perforations.
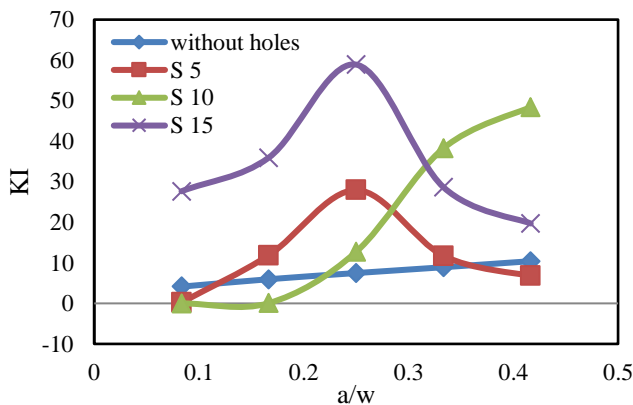

Fig. 33 Influence of crack length on the SIF in perforated plates with straight arrangement of rectangular perforations.
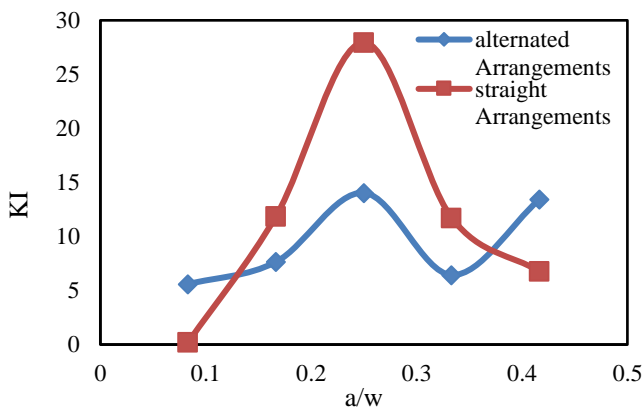

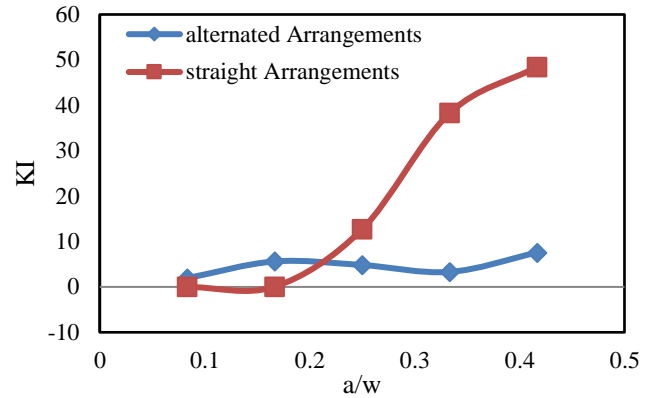**Fig. 34** Effect of arrangements of (S = 5 mm) on the SIF K_I

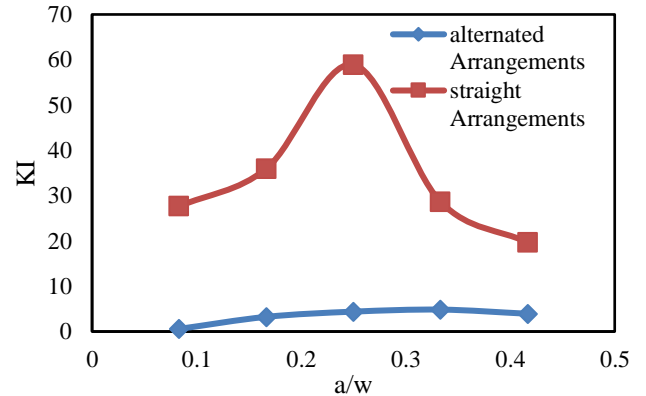**Fig. 35** Effect of arrangements of (S = 10 mm) on the SIF K_I

Fig. 36 Effect of arrangements of (S = 15 mm) on the SIF K_I

The effect of the shape factor for different size of rectangular perforation is represented in Fig. 37 that obtained using the Eq. (13) and CURVEEXPERT software program for the alternated arrangement of the perforations with correlation factor 78.2 % presented in Eq. (13). It is noted that from figures that the smaller the diameter of the holes, the higher shape factor value, this refers to the alternated arrangement of perforations. Fig. 38 show the effect of holes size on the values of geometry factor Y in the straight arrangement of perforations. It is observed that from this figure it is opposite of the alternate arrangement, where the smaller the diameter of the holes, the smaller the shape factor value. Eq. (14) represent the formulation of the shape factor Y for the straight arrangement that also obtained by CURVEEXPERT PROFESSIONAL with correlation factor 84.2 %.

$$Y((a/w), S) = -8344.51 + 26.71\,(a/w) - 113.378\,(a/w)^2 + 142.79\,(a/w)^3 + 3059.7\,(S) - 333.8\,(S)^2 + 11.127\,(S)^3 \qquad (13)$$
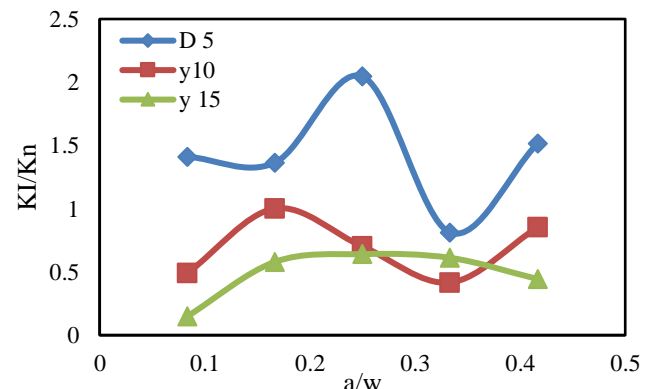

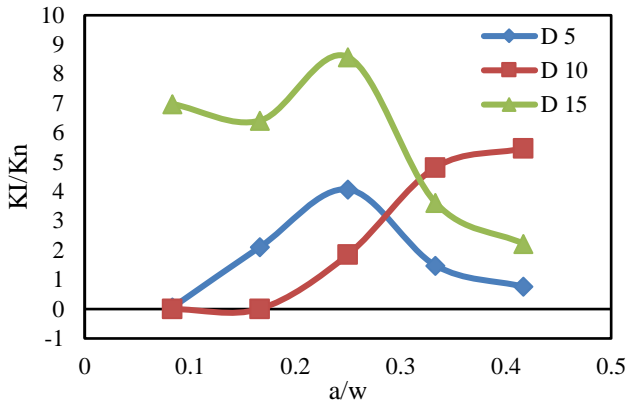**Fig. 37** Effect of crack length on shape factor Y for the alternate arrangement holes.

Fig. 38 Effect of crack length on shape factor *Y* for the straight arrangement.

$Y((a/w), S) = -27152.22 - 44.183 \, (a/w) - 21.66 \, (a/w)^2$
$- 64.61 \, (a/w)^3 - 9957.04 \, (S) - 1086.49 \, (S)^2$
$+ 36.226 \, (S)^3 + 18.4 \, (a/w)(S) + 1.35 \, (a/w)^2(S) +$
$- 1.03 \, (a/w)(S)^2$
$\hspace{10cm}(14)$

The equations (13) and (14) are available when (S = 2*r*) and the distance between holes equal to (*r*).

In order to investigate the effect of perforations type on the values of the stress intensity factor, Figs 39 and 40 represent the curves of the relation between the SIF values and (a/w) for the different three perforation shapes which are (circular, square, and rectangular perforations) in alternated and straight arrangement respectively in the presence of edge crack for each case with five different crack length (10 to 50 mm) with step (10 mm). It is noted that from this figure that the stress intensity factor values are increasing significantly when make a perforation plate with circular holes, while the rhombus holes also lead to increase the SIF values but with less effect than of the circular holes. In the case of rectangular perforations, the stress intensity factor values are increases significantly in both cases of the hole's arrangements and greater than the values in the circular and rhombus perforations. In general, the perforation geometry and arrangement have been affected on the elastic properties of the plate which in turn effect on the values of the stress intensity factor, while the cutting holes lead to a decrease in the weight of the plate and this will cause a reduction of the mass moment of inertia value, which in turn leads to a reduction in the stiffness of the plate. Additionally, the holes will alter the stress distribution in the plate, so the stress concentration may increase in certain areas and decrease in others. Therefore, the SIF will be different with the changing of crack length. So, at the areas with less stress concentration, the SIF will decrease and vice versa.
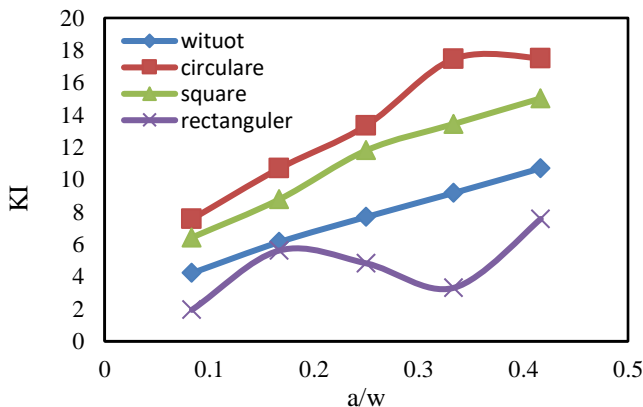

Fig. 39 Effect of crack length on the SIF in perforated plate with alternated arrangements and different perforation type.
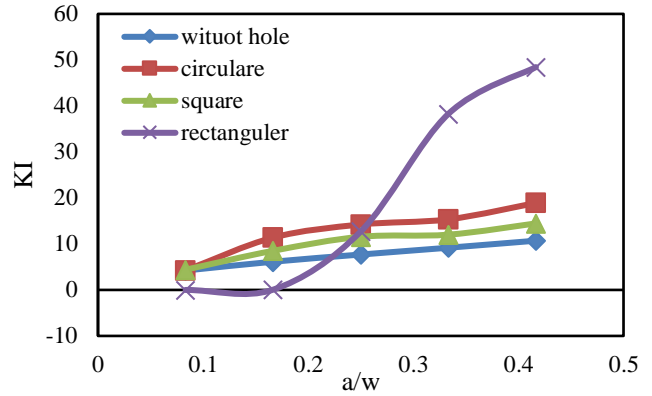

Fig. 40 Effect of crack length on the SIF in perforated plate with straight arrangements and different perforation type.

7. Conclusions

In this study, the extended finite element methods (XFEM) are used to determine the values of the stress intensity factor (KI) and shape factor (Y), for metal perforated plates with deferent of shapes and size of perforation, that loaded with uniaxial tension, and the following results were obtained:

1. In the case of circular holes, the increases in the average value of (SIF) reached to (80.88 %) when the plate was perforated with alternated arranged of circular holes, while in case of the straight arrangement of circular holes the increases of average values of SIF reach to (67.55 %).
2. As the case of rhombus holes, the stress intensity factor increases to (51.07 %) when the plate was perforated with alternated arrangement, while in the straight arrangement of holes the (SIF) increase to (35.43 %).
3. When the plate perforated with rectangular holes, the stress intensity factor values have been observed, a decrease in the values to (36.95 %) for the alternated arrangements of the holes.
4. The higher values of stress intensity factor obtained when the plates were perforated with circular holes, due to the circular shape that has more stiffness, so the absorption of force will be small compared with the rhombus and rectangular shape that will be less stiffness, which the absorption of strength is greater so, the stress concentration on the crack tip will be less.
5. It was observed through this study, the increases of stress intensity factor and the shape factor with different crack length were more stable in plate that perforated with alternated arrangement of holes than the straight arrangement.

References

[1] Goldberg, John Edward, and K. N. Jabbour "Stresses and displacements in perforated plates", Nuclear Structural Engineering, Vol. 2, No. 4, pp. 360-381, 1965.
[2] Cirello, Antonino, Franco Furgiuele, Carmine Maletta, and Antonino Pasta, "Numerical simulations and experimental measurements of the stress intensity factor in perforated plates", Engineering Fracture Mechanics, Vol. 75, No. 15, pp. 4383-4393, 2008.
[3] Webb, D. C., K. Kormi, and S. T. S. Al-Hassani, "Use of FEM in performance assessment of perforated plates subject to general loading conditions", International

Journal of Pressure Vessels and Piping, Vol. 64, No. 2, pp. 137-152, 1995.

[4] Chauhan, Mihir M., Dharmendra S. Sharma, and Jatinkumar M. Dave, "Stress intensity factor for hypocycloidal hole in finite plate", Theoretical and Applied Fracture Mechanics, Vol. 82, pp. 59-68, 2016.

[5] Bailey, R. and R. Hicks, "Behaviour of perforated plates under plane stress", Journal of Mechanical Engineering Science, Vol. 2, No. 2, pp. 143-165, 1960.

[6] Moës, Nicolas, John Dolbow, and Ted Belytschko, "A finite element method for crack growth without remeshing", International Journal for Numerical Methods in Engineering, Vol. 46, No. 1, pp. 131-150, 1999.

[7] Sukumar, Natarajan, Nicolas Moës, Brian Moran, and Ted Belytschko, "Extended finite element method for three-dimensional crack modelling", International Journal for Numerical Methods in Engineering, Vol. 48, No. 11, pp. 1549-1570, 2000.

[8] Stazi, F. L., Elisa Budyn, Jack Chessa, and Ted Belytschko, "An extended finite element method with higher-order elements for curved cracks", Computational Mechanics, Vol. 31, No. 1-2, pp. 38-48, 2003.

[9] Eftekhari, M., A. Baghbanan, and H. Hashemolhosseini, "Determining stress intensity factor for cracked brazilian disc using extended finite element method", International Journal of Scientific Engineering and Technology, Vol. 3, No. 7, pp. 890-893, 2014.

[10] Daux, Christophe, Nicolas Moës, John Dolbow, Natarajan Sukumar, and Ted Belytschko, "Arbitrary branched and intersecting cracks with the extended finite element method", International Journal for Numerical Methods in Engineering, Vol. 48, No. 12, pp. 1741-1760, 2000.

[11] Jiang, Shouyan, Zongquan Ying, and D. U. Chengbin, "The optimal XFEM approximation for fracture analysis", Materials Science and Engineering, Vol. 10, pp. 1-10, 2010.

[12] Khalaf, Hassanien I., "Crack Propagation in Plane Stress Problems by Using Experimental and Extended Finite Element Method (XFEM)", Ph.D. thesis, Mechanical Engineering Department, College of Engineering, University of Basrah, 2015.

[13] Schreurs, P. J. G, "Lecture notes-course 4A780 Concept version", Materials Technology, 2012.

[14] Nama, Sabreen Saad' "Investigation of Stress Intensity Factor for Corrugated Plates with Different Profiles Using Extended Finite Element (XFEM)", Ph.D. thesis, Mechanical Engineering Department, College of Engineering, University of Basrah, 2018.

[15] Laftah, Rafil Mahmood, "Study of Stress Intensity Factor in Corrugated Plate Using Extended Finite Element Method (XFEM)", Engineering and Technology Journal, Part (A), Vol. 34, No. 15, pp. 2982-2992, 2016.

[16] Nama, Sabreen Saad, and Rafil Mahmood Laftah, "Investigation of Stress Intensity Factor for Corrugated Plates with Different Profiles Using Extended Finite Element (XFEM)", Basrah Journal for Engineering Sciences, Vol. 18, No. 1, pp. 1-9, 2018.